Polymorphism of 1,2,3-trichloropropane: NQR and DTA study of the ordered and disordered phases

2004 J. Phys.: Condens. Matter 16 7873

(http://iopscience.iop.org/0953-8984/16/43/026)

INSTITUTE OF PHYSICS PUBLISHING JOURNAL OF PHYSICS: CONDENSED MATTER

J. Phys.: Condens. Matter **16** (2004) 7873–7887 PII: S0953-8984(04)81976-3

Polymorphism of 1,2,3-trichloropropane: NQR and DTA study of the ordered and disordered phases

N Veglio, M J Zuriaga[1] and G A Monti[1]

Facultad de Matemática, Astronomía y Física, Universidad Nacional de Córdoba, Medina Allende s/n, Ciudad Universitaria, X5016LAE Córdoba, Argentina

E-mail: zuriaga@famaf.unc.edu.ar

Received 10 June 2004
Published 15 October 2004
Online at stacks.iop.org/JPhysCM/16/7873
doi:10.1088/0953-8984/16/43/026

Abstract

1,2,3-Trichloropropane was investigated by means of nuclear quadrupole resonance (NQR) and differential thermal analysis (DTA). One amorphous state and two crystalline monotropic phases (forms I and II) were found depending on the thermal history of the sample and only one is stable up to the melting point. The different phases were characterized by ^{35}Cl NQR. It was concluded that form I is an ordered crystal with only one molecular conformation present in the unit cell while form II is a disordered state with at least two molecules present in the unit cell.

In the two crystalline phases, the presence of group reorientations ($-CH_2Cl$) and molecule reorientations as a whole can be inferred from ^{35}Cl spin–lattice relaxation times (T_1) with activation energies of 33 and 42 kJ mol^{-1}, respectively, in form I. In form II, these activation energies are in the range 20–29 kJ mol^{-1} indicating that this polymorph is less compactly crystalline packed in comparison to form I.

1. Introduction

Many chain organic compounds are capable of existing in more than one form in the solid state. Sometimes, the particular state assumed by the compounds depends not only upon the substance itself but upon its previous thermal history as well. Therefore, calorimetric and spectroscopic studies in a wide range of temperatures are necessary to characterize the transformations. Particularly, in compounds with one axis of symmetry, e.g. long-chain compounds such as $(CH_2)_n$ with $n > 2$, anisotropic orientational disorder has been observed [1], while orientational isotropic disorder is found in some short chains like $(CH_2Cl)_n$, which is typically found in substances composed of spherical molecules with unusually high mobility [2]. Until now, not much has been done in chains with n between 3 and 9. In the present work, we report the

[1] Fellow of CONICET.

studies carried out on 1,2,3-trichloropropane (TCP). This organic compound belongs to the family of halogenated propanes, and has previously been investigated by means of vibrational spectroscopy [3, 4] and gaseous electron diffraction [5]. The 1, 2, 3-trihalopropanes with identical halogens usually have six possible staggered conformations. It has been reported that in the liquid and gaseous phase only three rotational isomers are present (corresponding to the lowest energies) while only one survives after solidification to 200 K [6]. However, other authors reported the survival of two conformers in TCP at 90 K [7].

Nuclear quadrupole resonance (NQR) is a technique based on the interaction between the nuclear electric quadupolar moment and the electric field gradient (EFG) at the nuclear site [8]. Since the magnitude of the EFG at the nuclear site is an extremely sensitive function of its near-neighbour environment, NQR is an appropriate technique to characterize different solid phases and phase transformation [8]. In molecular crystals, the EFG at the nuclear site is determined both by a large intramolecular contribution, mainly due to electronic bonding, and a crystalline one, due to short-range intermolecular interactions, usually being less than 5% [9]. When some kind of disorder is present, the resonance line which reflects the local structural order is considerably broadened [10–14].

In this work TCP has been investigated analysing the temperature behaviour of NQR resonance frequency, line shape and ^{35}Cl relaxation times together with DTA measurements.

2. Experimental

TCP (Fluka, catalogue #91380) was used without further purification. High-resolution NMR spectra showed that impurities of $=CH_2$ and $-CH_3$ were less than 1%. The sample was placed in glass ampoules and sealed under vacuum.

The ^{35}Cl NQR transition frequencies and spin relaxation times (T_1 and T_2), were measured by means of a fast Fourier transform (FFT) pulsed spectrometer. The NQR signal was detected by the Hahn echo sequence [15] ($\pi/2 - \tau - \pi$) with a $\pi/2$ pulse of 10 μs. The absorption line shape, in the ordered crystalline phase was obtained from the FFT of the echo. To obtain the NQR spectra in the amorphous state and in the form II, the nuclear spin-echo Fourier transform mapping spectroscopy (NSEFTMS) method [16] was used. To obtain the mapped spectrum, the following parameters were used, $\pi/2$ pulse 10 μs, which correspond to a value for $\nu_1 = \omega_1/2\pi$ of about 25 kHz. The value of τ was set to 80 μs, i.e. such that $\tau \gg T_2^*$, in order to eliminate distortions from the FID of the second pulse. The other parameters were set as follows: number of scans 1000, acquisition time for each spin-echo 500 μs, mapping step 26 kHz ($\approx \nu_1$) and the number of sampling frequencies 40. To get the NQR parameters as a function of the temperature in the disordered phases, the sample was quenched to liquid nitrogen temperature. Then it was heated up to the desired temperature at heating rates less than 1 K min^{-1} and after stabilization for 1 h, the corresponding measurements were performed. This whole process was repeated to record the NQR measurements for each temperature.

The spin–lattice (T_1) and spin–spin (T_2) relaxation times were measured by using the inversion-recovery ($\pi - \tau - \pi/2$) and the Hahn-echo sequences, respectively. The temperatures were measured with copper–constantan thermocouples to an accuracy of ± 0.2 K, while the stability during the NQR measurements was better than ± 0.1 K.

The DTA runs were recorded with an improved home-made apparatus [17] with heating rates between 0.1 and 0.5 K min^{-1}. The DTA experiments were carried out on a specimen that was cooled down to approximately the liquid-nitrogen temperature in two different ways: (i) slow cooling at a rate of 0.25 K min^{-1}, and (ii) rapid cooling from the liquid state at room temperature down to 77 K by plunging the specimen into liquid nitrogen.

The same sample was used in both the DTA and the NQR measurements.

3. Results and discussion

3.1. DTA studies

The DTA heating traces are shown in figure 1. In the slowly cooled sample only an endothermic peak due to melting appears at $T_m = 259\ K$ (figure 1(a)). From figure 1(b) we can see that quenching of the sample produces a vitreous state. At about 140 K a step change of ΔT appears. This change is associated to a heat capacity jump [18] which is typical for a glass transition [19].

A glass temperature $T_g = 146$ K was determined from the DTA traces by the usual methods [18]. At about 155 K, the specimen undergoes a spontaneous change with evolution of heat that is associated to the crystallization of the supercooled liquid into a solid form. As will be shown later, from the NQR data analysis we conclude that this form II is not the same form obtained by slow cooling of the sample. Depending on the heating rate, one or two exothermic peaks, with smaller enthalpy changes, appear at about 170 and 180 K. These exothermic peaks correspond to a solid–solid transformation from the crystalline form II to form I probably through an intermediate phase. The endothermic peak at 259 K is the melting of this latter form.

The warming curve obtained for the slowly cooled sample shows the melting peak at the same temperature as that obtained after quenching, indicating that in the two cases TCP was in the crystalline form I before melting. Melting of form II was never observed.

The solid–solid transitions observed are exothermic indicating that the transitions are monotropic [20], with form II being the metastable form and form I the stable one.

Figure 2 shows the DTA traces obtained from the fast-cooled sample at heating rates of 0.1 and 0.5 K min^{-1}. The transition temperatures $T_{\rm g}$, $T_{\rm x}$ and $T_{a,b}$ shift to higher temperatures with increasing heating rates, indicating the kinetic nature of the transitions.

DTA studies allowed us to conclude that, between 77 and 270 K, TCP can exist in one amorphous state ($T < 146$ K) and at least two monotropic phases (form II below 180 K and form I above 77 K).

3.2. NQR studies

The NQR spectrum of crystalline form I was obtained on heating from a slow-cooled sample. This spectrum exhibits three lines (ν_α, ν_β, ν_γ) of the same intensity and width (~ 5 kHz), associated to each chlorine in the molecule. Therefore, all the molecules in the unit cell are equivalent. Their temperature dependences (ν_Q versus T), in the range 80–260 K [6], are depicted in figure 3. The linewidth values are typical of an ordered phase and increase near the melting point due to the presence of a thermally activated process observed in the behaviour of the relaxation times (figure 8) [8].

Figure 4 shows the evolution of the NQR spectrum in the rapidly cooled sample as the temperature is increased from 77 to 200 K. A very broad line with some structure is observed at low temperatures. When the temperature is increased further, four clearly distinguishable broad resonance peaks become visible and above 170 K three narrow lines of form I are observed.

Figure 5 shows a deconvolution of the NQR spectrum between 100 and 160 K. For temperatures between 77 K and T_g one Gaussian line and four Lorentzian lines are enough to get a good fit of the spectra. It is clear from the evolution of the peak area that the Gaussian line fades out at a temperature around T_g, while the area of the four Lorentzian peaks remain constant up to approximately T_x. The broad Gaussian line is associated to the amorphous state observed by DTA measurements. The four broad Lorentzian peaks ($\Delta\nu \simeq 70$ kHz) are associated with the crystalline form II. Their intensities, corrected for T_2 relaxation effects,

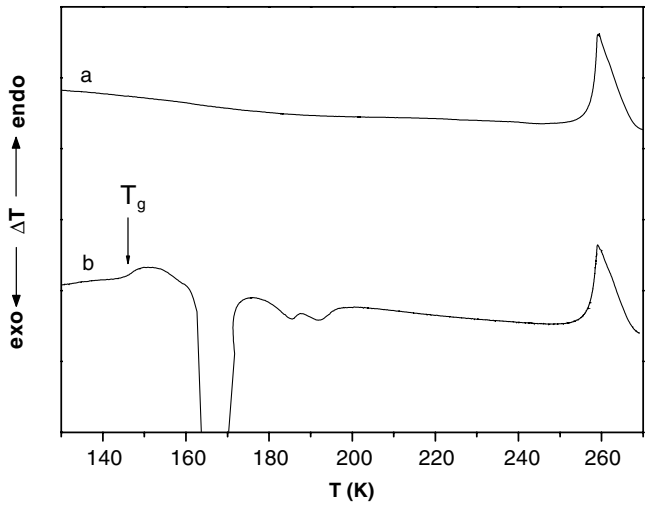

Figure 1. DTA heating runs for TCP. Traces a and b are obtained by slowly cooling down the sample and quenching into liquid nitrogen, respectively. As is clearly shown, for the slowly cooled sample, the only anomaly in the specific heat is that corresponding to the melting. On the other hand, for the fast-cooled sample, new phases are obtained at liquid nitrogen temperature and on heating up from that point.

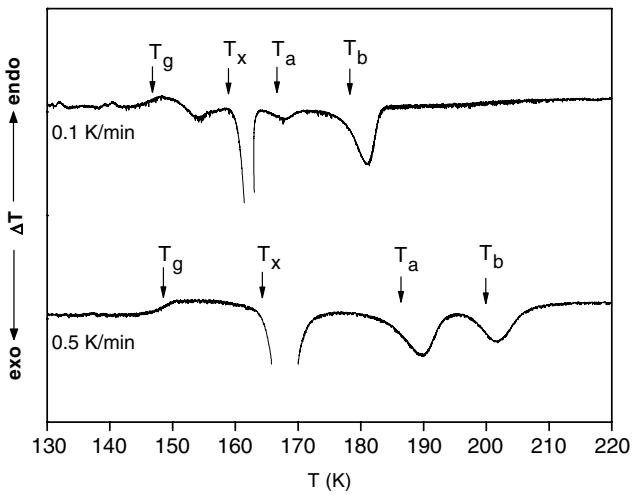

Figure 2. DTA traces obtained for a fast-cooled sample, at heating rates of 0.1 and 0.5 K min^{-1}. The kinetic nature of the transitions is clearly observed.

are in the ratio 1 : 1 : 2 : 2. Since the molecule has three non-equivalent chlorine nuclei, there have to be at least two non-equivalent molecules in the unit cell in order to account for the number of lines and intensity ratios. The temperature dependences of the NQR frequencies corresponding to the four Lorentzian peaks ($\nu_1, \nu_2, \nu_3, \nu_4$) are depicted in figure 3. From the resonance linewidth ($\Delta\nu \simeq 70$ kHz), it can be concluded that form II is orientationally and/or

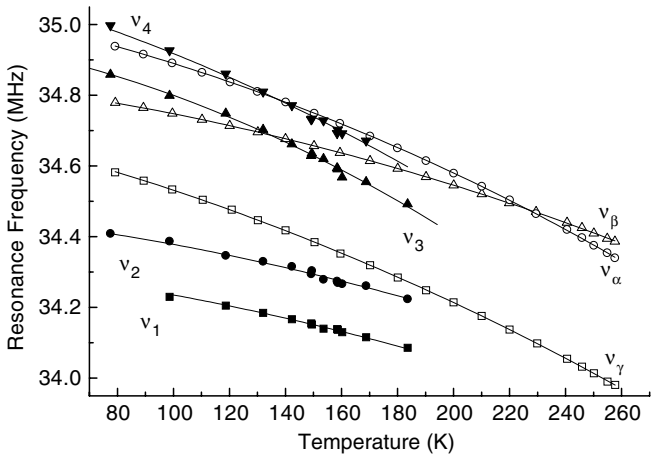

Figure 3. Temperature dependences of the NQR transition frequencies for TCP. Lines α, β, and γ correspond to Cl(3), Cl(2) and Cl(1), respectively, in the only crystalline phase obtained by slow cooling of the sample. Lines 1, 2, 3 and 4 are the transitions obtained for the crystalline phase of the fast-cooled specimen (form II). The full lines represent the description obtained of the various transitions by using equation (1) with the parameters given in [6] for TCP.

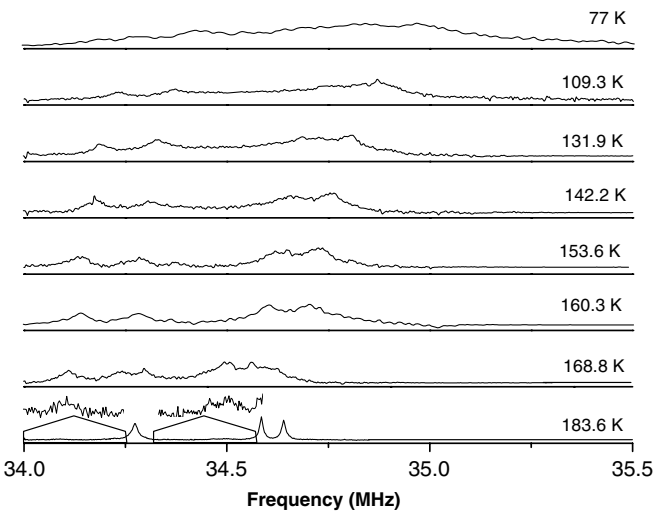

Figure 4. Temperature dependence of the NQR spectrum for the fast-cooled TCP sample. Expansions of the spectrum at 183.6 K show the presence of the NQR lines corresponding to form II at that temperature.

conformationally disordered [11, 21]. It should be noted that the NQR lines of the crystalline form II appear in the temperature region corresponding to the amorphous state. It is assumed that this is because, in the quenching process, the entire sample does not reach the amorphous state, some of it goes to form II. This fact is in agreement with Ostwald's step rule [22] that states that the initially formed state is the least stable state lying nearest in free energy to the original state. Figure 6 shows the temperature dependence of the total lines area in each phase. It is observed that between 77 K and T_g the signal of the amorphous state fades out while the

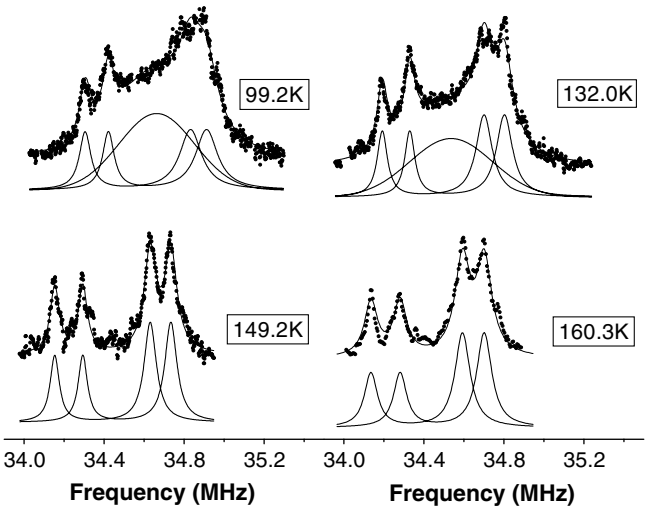

Figure 5. Deconvolution of the NQR spectra at different temperatures. Solid lines are the fitted resonances (four Lorentzian lines and one Gaussian line). Squares are the experimental data. The decrease in intensity of the resonance corresponding to the amorphous phase (broader line) with an increase in temperature from 99 to 149 K is clearly seen.

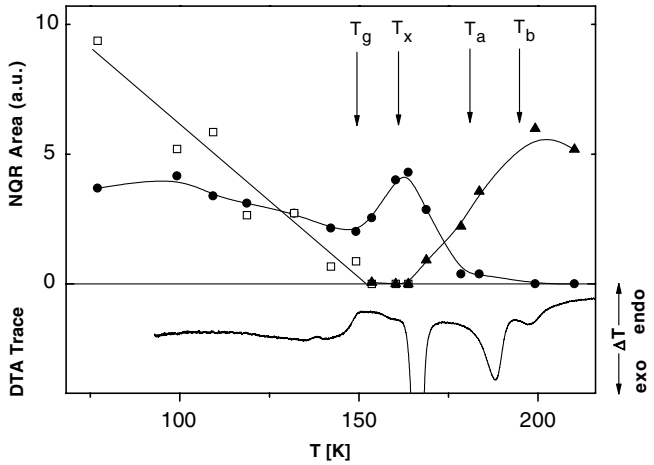

Figure 6. Temperature dependence of the total area of the NQR resonance lines. □, for the amorphous phase; ●, form II; ▲, form I. The solids lines are just a guide to the eyes. For comparison, a DTA heating run for a fast-cooled specimen is shown.

signal of form II remains constant. At T_x the amorphous state crystallizes in form II. Between T_a and T_b form I begins to appear and at T_b form II disappears.

We should note here that in the temperature range $T_a < T < T_b$, no different phase was detected by means of NQR. However, since the presence of one or two exothermic transitions around 170–180 K in DTA measurements is a fact that depends on the kinetics of the experiment, we cannot discard the existence of a third polymorphic form in that temperature range.

Due to the averaging effect of the molecular vibrations on the EFG, the quadrupolar resonance frequency decreases as the temperature is increased. The normal temperature dependence of the resonance frequency may be accounted for by the Bayer–Kushida theory [23]. The temperature behaviour of ν_Q is mainly driven by the librational motions of the molecule as a rigid body and may be described to a good approximation by the following expression:

$$\nu_Q = \nu_{Q0}\left\{1 - \frac{3h}{8\pi}\frac{A_l}{\omega_l}\coth\left(\frac{h\omega_l}{4\pi k_B T}\right)\right\}. \tag{1}$$

Here the ν_{Q0} are the rigid lattice NQR frequencies, $\omega_l = \omega_{l0}(1 - g_l T)$ is an effective librational frequency [23, 24], A_l is the inverse of the effective moments of inertia for the corresponding normal modes [6]; h and k_B have their standard meanings.

In several orientationally or substitutionally disordered molecular crystals, the character and the frequency of the lattice modes are similar to that of the ordered crystal [25–27]. Under this assumption, equation (1) can also be used to describe the temperature dependence of the NQR frequency in form II.

In a previous work it has been shown that in form I ν_α and ν_γ are associated to the Cl(3) and Cl(1), respectively, and ν_β to the central chlorine Cl(2), as shown in figure 7 [6]. An assignment can be also made in form II. The lines are labelled ν_1, ν_2, ν_3 and ν_4 in the order of increasing frequency (figure 3). The temperature dependence of ν_1 and ν_2 is very similar to that of line ν_β in form I while the temperature behaviour of ν_3 and ν_4 is very similar to the corresponding behaviour of lines ν_α and ν_γ, respectively. For this reason it is possible to assume that the molecular structure is the same in both phases and assign to lines ν_3 and ν_4 the value $A_e^{\alpha,\gamma}$ calculated for lines ν_α and ν_γ and the value A_e^β of line ν_β to lines ν_1 and ν_2.

A least-squares fit of equation (1) to the ν_Q data yields the values for the parameters ω_{l0} and g_l shown in table 1, where the calculated values of A_l from structural data were used [5] (i.e. $A_e^{\alpha,\gamma} = 4.75 \times 10^{-3}$ (amu Å^2)$^{-1}$ and $A_e^\beta = 4.75 \times 10^{-3}$ (amu Å^{-2})$^{-1}$).

A comparison of the parameters shown in table 1, and the fact that the intensity rates of the resonance lines in form II are 1 : 1 : 2 : 2, allow us to conclude that resonance line ν_β in form I is split into lines 1 and 2 of form II. No Raman and infrared data are available for the solid in the region of the lattice modes; however, the values for the mean librational frequencies and their temperatures coefficients are in agreement with typical values for this kind of compound. Also, in the two phases, the effective librational frequencies are equal within the experimental error indicating that the vibrational spectra in form I and form II are not very different.

Finally, the spin–lattice relaxation time T_1, and the spin–spin relaxation time T_2, were measured from 80 to 260 K for all three resonance lines of form I, and from 80 to 170 K for all four resonance lines of form II in TCP. The results are shown in figures 8 and 9. It is important to notice here that for temperatures lower than T_g, the time dependence of the magnetization $S(\tau)$ after saturation is two-exponential (see figure 10). This is consistent with the assumption that for $T < T_g$ the amorphous state coexists with form II. The short relaxation time (~ 10 ms) is associated to the chlorine atoms in the amorphous phase. This value is considerably shorter than the T_1 in crystalline phases at the same temperature indicating a relaxation mechanism more efficient than the lattice vibrations. Two well-defined temperature regions may be distinguished for all three lines of form I. Below 200 K, T_1 behaves normally, indicating that the dominant relaxation mechanism is due to librational modes. Above this temperature, a dramatic shortening of T_1 occurs, indicating the onset of a very efficient thermally activated process. At temperatures lower than 230 K, T_2 remains constant with the temperature. For

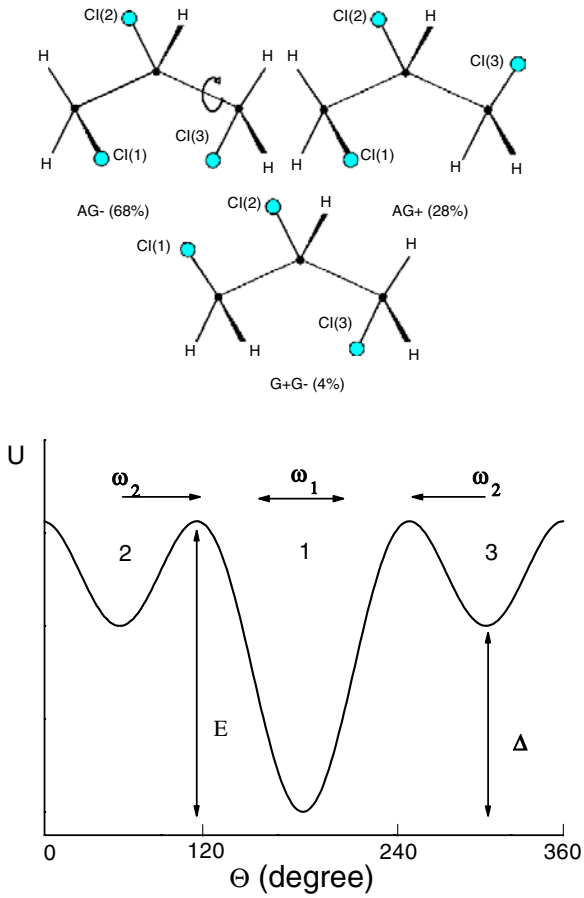

Figure 7. Upper panel: the TCB molecule in the different configurations. Lower panel: the proposed potential felt, and the meaning of the various parameters used, by the $-CH_2Cl$ end groups in order to carry on reorientations of $\pi/3$ about the C–C axis as is shown in the upper panel. ω_1 and ω_2 are the jump frequencies through wells of height E and $E - \Delta$, respectively.

(This figure is in colour only in the electronic version.)

Table 1. Values obtained for the parameters by fitting equation (1) to the frequency data.

Parameter	$\omega_{0l}/2\pi$ (cm^{-1})	g_l (cm^{-1} K^{-1}) $\times 10^{-4}$
TCP form I		
ν_β	103 ± 1	7.7 ± 1
$\nu_{\alpha,\gamma}$	74 ± 1	7.3 ± 0.2
TCP form II		
$\nu_{1,2}$	107 ± 9	8 ± 3
$\nu_{3,4}$	68 ± 5	8 ± 3

temperatures above 230 K, the shortening of T_1 dominates the T_2 behaviour. A similar T_1 versus T behaviour was found for all four lines in form II. The values of T_2 for this form remain constant over all the temperature range and they are about one half of the T_2 values of form I.

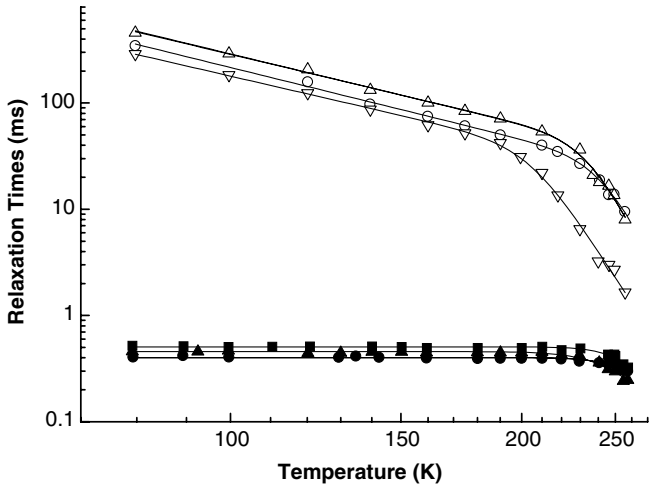

Figure 8. Temperature dependences of the NQR relaxation times for TCP slow-cooled sample, T_1 (open symbols) and T_2 (close symbols). Circle, up triangle, and down triangle correspond to transitions frequencies α, β, and γ shown in figure 3, respectively. The onset of a thermally activated process is clearly seen. The T_1 full lines are the description provided by equation (2) with the parameters shown in table 2.

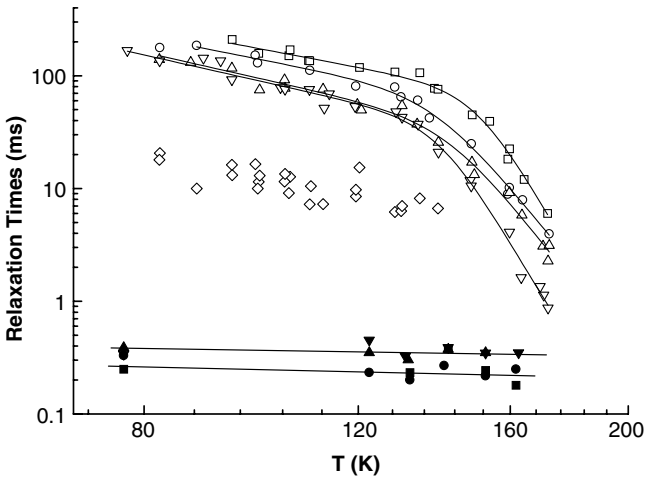

Figure 9. Temperature dependences of the NQR relaxation times for TCP fast-cooled sample at T_1 (open symbols) and T_2 (close symbols). Square, circle, up triangle, and down triangle correspond to transitions frequencies 1, 2, 3, and 4 shown in figure 3, respectively. $\diamond$, T_1 relaxation time behaviour of the amorphous phase. The onset of a thermally activated process is clearly seen. The T_1 full lines are the description provided by equation (2) with the parameters shown in table 2.

The relaxation time may then be described by the following equation:

$$T_1^{-1} = aT^{\lambda} + b\exp(-E_a/RT). \tag{2}$$

The first term on the right-hand side of equation (2) represents the contribution from lattice vibrations [8] and the second term corresponds to a thermally activated process [23, 28],

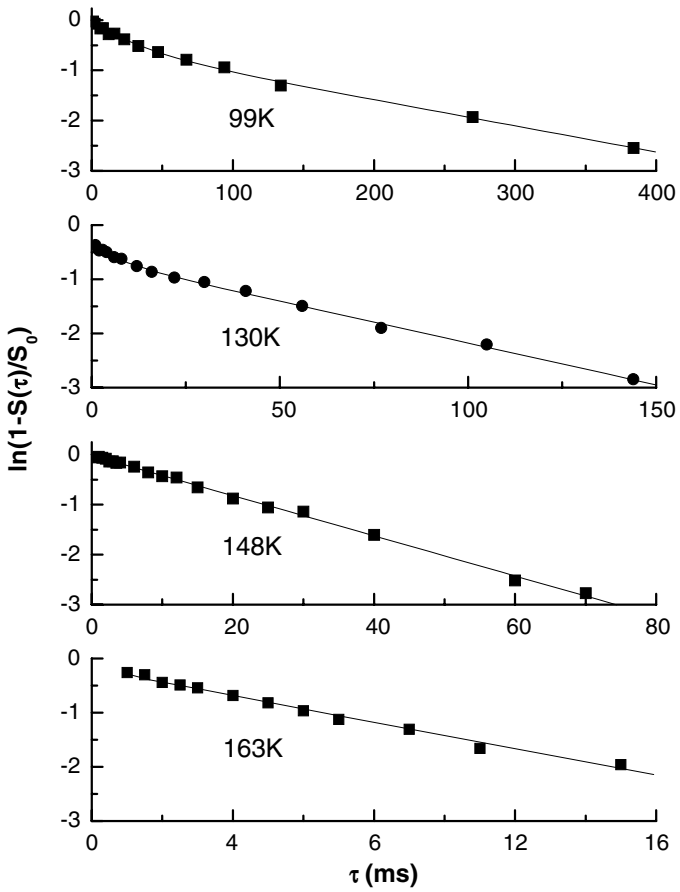

Figure 10. Two-exponential time dependence of the magnetization $S(\tau)$ at temperatures lower than T_g for the fast-cooled TCP sample. This is consistent with the assumption that for $T < T_g$ the amorphous state coexists with form II. The short relaxation time ($\sim$10 ms) is associated to the chlorine atoms in the amorphous phase. When the temperature is close to T_g relaxation becomes single exponential.

which for the present case are due to reorientations of the molecule or molecular fragment (CH_2Cl). E_a corresponds to the activation energy and the pre-exponential factor depends on the relaxation mechanism: $b \sim \omega_0$ for self-reorientations and $b \sim (q'/q)^2\tau_0^{-1}$ for modulation of the EFG due to reorientations of neighbouring molecules or groups [13, 29]. Here q' is the fraction of the EFG produced at the observed nucleus by the moving group and q is the z-component of the total EFG tensor at the observed nucleus. The best-fit parameters λ and E_a were determined by using non-linear least-squares methods and are shown in table 2. The λ values are very similar for all the resonance lines in the two crystalline forms, as expected from the relaxation mechanism driven by lattice vibrations.

TCP has asymmetric tetrahedral molecular fragments of the type MXY_2. The reorientation takes place between equilibrium sites corresponding to unequal minima of the molecular potential energy. The form of the reorientational potential energy function used to describe the dynamics of the fragments $–CH_2Cl$ and the various characteristic parameters are depicted in figure 7.

Table 2. Parameters obtained by fitting equation (2) to the T_1 versus T data.

Parameter	λ	b^{-1} (10^{-10} s)	E_a (kJ mol^{-1})
TCP form I			
ν_α	2.1 ± 0.1	10	33 ± 2
ν_β	2.1 ± 0.1	0.3	42 ± 4
ν_γ	2.2 ± 0.1	0.7	42 ± 4
TCP form II			
ν_1	2.0 ± 0.4	0.2	29 ± 5
ν_2	2.1 ± 0.5	40	20 ± 2
ν_3	2.4 ± 0.3	12	21 ± 2
ν_4	2.4 ± 0.2	0.1	26 ± 2

Ainbinder *et al* [29] have analysed the slow reorientations of a molecular group containing quadrupolar nuclei between the three wells shown in figure 7. They conclude that the temperature dependence of T_1 (equation (2)), when $\Delta \gg RT$, gives the value of the smaller potential barrier $E - \Delta$. A reanalysis of this model has been made under more realistic experimental conditions. It was found that the parameter E_a in equation (2) corresponds to the activation energy E for transitions of the molecule from the equilibrium ground-state position to the other ones. The details of this calculation are shown in the appendix.

As was mentioned before, TCP has six possible staggered conformations. They are named A (anti) and G (gauche) according to the position of the neighbouring chlorines [3]. Of these theoretical conformers, three have been detected in TCP in the vapour phase [5] with relative concentrations of 68, 28 and 4% for AG−, AG+ and G+G−, respectively, and they are shown in figure 7. For a TCP molecule, a $\pi/3$ rotation of the –$CH_2Cl(3)$ group in the AG− conformer about the axis C(2)–C(3) leads to the AG+ conformer, and a similar rotation of the $CH_2Cl(1)$ to the G+G−. Since G+G− is energetically less favourable than the AG+ configuration [3–5], it is reasonable to expect that the activation energy for the reorientation of the $CH_2Cl(3)$ group will turn out to be smaller than that for the $CH_2Cl(1)$ group. These analyses are in excellent agreement with the results shown in table 2 for the case of crystalline form I. The Cl(2) nucleus also goes through a thermally activated process. We must discard the modulation effect of the EFG at the site of this nucleus due to reorientation of the $-CH_2Cl$ end groups, as responsible for the sharp decrease in T_1. In the case of modulation, the value of the pre-exponential coefficient b in equation (2) can be evaluated using q' proportional to the inhomogeneous linewidth [13] ($\Delta\nu \simeq 10$ kHz in form I and $\Delta\nu \simeq 70$ kHz in form II). As a result of this, b should be several orders of magnitude smaller than that obtained in the case of molecular reorientations [8]. A plausible explanation for these observations is as follows: the reorientation of the $CH_2Cl(3)$ group, with an $E_a = 33$ kJ mol^{-1}, is the first to be detected that gives place to the shortening of T_1^α; at higher temperatures, the reorientation of the molecule as a whole, with $E_a = 42$ kJ mol^{-1}, begins to be the most effective relaxation mechanism for the three lines. Within the experimental uncertainty, it is not possible to distinguish the different processes on the line ν_α.

As was mentioned above, the T_1 temperature behaviour of form II is very similar to that of form I. Activation energy values in the range 20–29 kJ mol^{-1} were found by fitting equation (2) to the experimental data. These values are slightly smaller than the values found for form I. This fact suggests that crystalline form II is less compactly packed than form I. In this case, due to the dispersion of the E_a values and to the existence of many non-equivalent molecules in the unit cell, an interpretation of the results as for form I it is not possible.

4. Conclusions

In the temperatures range 77–270 K, one amorphous phase and at least two crystalline monotropic forms were found in 1, 2, 3-trichloropropane. By a fast cooling down of the sample, from a room temperature liquid state to a liquid-nitrogen temperature, an amorphous state is obtained that, on heating, crystallizes into a metastable form (form II). Form II is a disordered phase, with at least two unequivalent molecules in the unit cell, due to the fact that probably two conformers are present in the unit cell. This is in a good agreement with the presence of two conformers reported by other authors at 90 K [7]. At 180 K, the transition to the stable phase (form I) is observed. Form I is an ordered phase with only one molecular conformation present in the unit cell, also in good agreement with the report of Thorbjönsrud *et al* [3]. At slower cooling rates, only the stable crystalline phase is obtained on cooling.

Two relaxation mechanisms, in the high-temperature range, are distinguished in TCP form I, i.e. the reorientational motions of the $-CH_2Cl(3)$ end groups and the reorientation of the molecule as a whole. Activation energies of 33 and 42 kJ mol^{-1} respectively, were obtained for those mechanisms. In form II there are also molecular reorientations but with activation energies appreciably lower than in form I.

It has also been shown that, in the case of slow reorientation of a molecular group of the form MXY_2, between unequal potential wells of the form shown in figure 7, the temperature dependence of T_1 measurements only gives information on the higher potential barrier value.

Acknowledgments

Partial financial support provided by CONICET (Consejo Nacional de Investigaciones Científicas y Técnicas), and SECyT UNC (Secretaría de Ciencia y Técnica de la Universidad Nacional de Córdoba) is gratefully acknowledged.

Appendix

We will analyse the slow reorientations of the molecular group containing a quadrupolar nucleus (CH_2Cl) between the three wells shown in figure 7. The evolution of the occupation number of the eigenstate m of the quadrupolar Hamiltonian, at the site ν, n_m^ν, is given by [28]

$$\frac{\partial n_m^\nu}{\partial t} = \sum_{\nu'} \sum_n (p_{mn}^{\nu\nu'} n_n^{\nu'} - p_{nm}^{\nu'\nu} n_m^\nu),$$

where $P_{mn}^{\nu\nu'}$ are the transition probabilities from the n state in the site ν', to the m state in the site ν.

For spin $I = 3/2$, the spin polarization at the site ν can be written as

$$P^\nu = n_{3/2}^\nu + n_{-3/2}^\nu - n_{1/2}^\nu - n_{-1/2}^\nu. \tag{A.1}$$

For a molecular fragment of the type MXY_2 in the potential shown in figure 7, the evolution equation for the nuclear polarization (equation (A.1)) can be written as [28, 29]

$$\frac{\partial \vec{\mathbf{P}}}{\partial t} = R\vec{\mathbf{P}}, \tag{A.2}$$

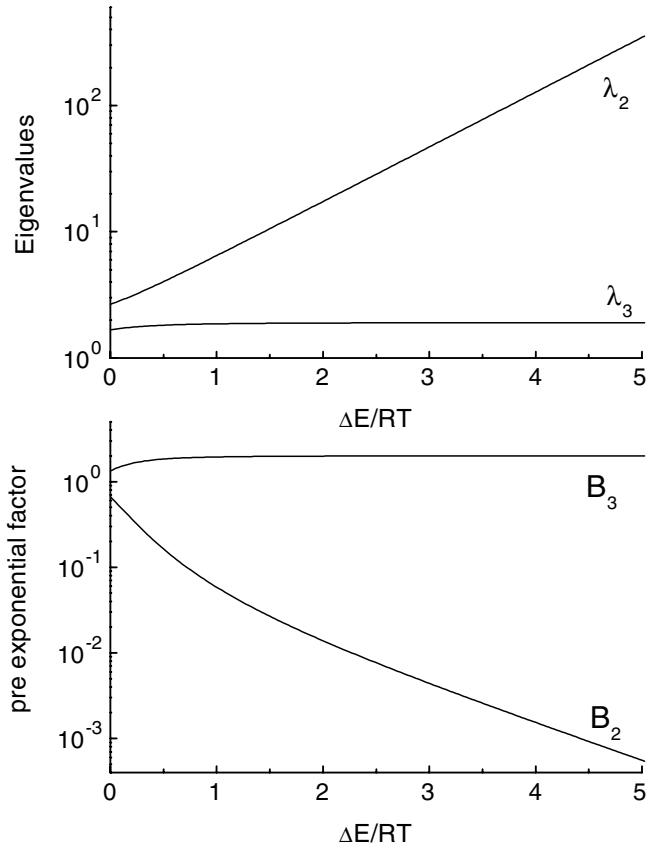

Figure A.1. Dependences of the spin–lattice relaxation times $T_1^1 = (\lambda_2)^{-1}$ and $T_1^2 = (\lambda_3)^{-1}$ on the parameter $\alpha = \Delta/RT$ are shown. As may be seen, as soon as $\alpha > 1$, i.e. for $\Delta > RT$, the coefficient B_2 decreases exponentially, while the value of B_3 remains approximately constant with α. Therefore the second term on the right-hand side of equation (6) is the dominant one and the relaxation of the nuclear polarization can be described by a single exponential decay curve.

with

$$\vec{\mathbf{P}} = \begin{pmatrix} P^1 - P_0^1 \\ P^2 - P_0^2 \\ P^3 - P_0^3 \end{pmatrix} \qquad \text{and} \qquad R = \begin{pmatrix} -2\omega_1 & -\frac{1}{3}\omega_2 & -\frac{1}{3}\omega_2 \\ -\frac{1}{3}\omega_1 & -2\omega_2 & -\frac{1}{3}\omega_2 \\ -\frac{1}{3}\omega_1 & -\frac{1}{3}\omega_2 & -2\omega_2 \end{pmatrix},$$

where $\nu = 1, 2, 3$ stands for the three minima of the potential, P_0^ν is the thermal equilibrium nuclear polarization, R is the relaxation matrix, $\omega_1 = \omega_0 \exp(-E/RT)$ and $\omega_2 = \omega_0 \exp[-(E - \Delta)/RT]$ are the jump frequencies as indicated in figure 7.

In an earlier work [29] it was assumed that the observed NQR signal is the sum of the nuclear polarization at each site, i.e. $P = P^1 + P^2 + P^3$. This is valid if all of the sites are equivalent but, if they are not, then the NQR signal will be different [6, 30]. In the present case, the three equilibrium sites are not equivalent. Only one signal is observed from each (CH_2Cl) group. The observed NQR signal comes from the chlorine atoms at the lowest minimum, $\nu = 1$, and because the population rate between unequal potential wells is

$Population_1/Population_{2,3} = \exp(\Delta/RT)$, this fact indicates that $\Delta/RT \gg 1$. Hence we need to solve equation (A.2) with suitable initial conditions.

The eingenvalues, λ_i, and eigenvectors, $\vec{A}_i$, of the relaxation matrix are

$$\lambda_1 = \tfrac{5}{3}\omega_2, \qquad \lambda_2 = \omega_1 + \tfrac{7}{6}\omega_2 + \sqrt{(\omega_1 - \tfrac{7}{6}\omega_2)^2 + \tfrac{2}{9}\omega_1\omega_2},$$

$$\lambda_3 = \omega_1 + \tfrac{7}{6}\omega_2 - \sqrt{(\omega_1 - \tfrac{7}{6}\omega_2)^2 + \tfrac{2}{9}\omega_1\omega_2},$$

$$\vec{A}_1 = \{0, -1, 1\},$$

$$\vec{A}_2 = \left\{ \frac{\omega_1 - \frac{7}{6}\omega_2 + \sqrt{(\omega_1 - \frac{7}{6}\omega_2)^2 + \frac{2}{9}\omega_1\omega_2}}{\frac{1}{3}\omega_1}, 1, 1 \right\},$$

$$\vec{A}_3 = \left\{ \frac{\omega_1 - \frac{7}{6}\omega_2 - \sqrt{(\omega_1 - \frac{7}{6}\omega_2)^2 + \frac{2}{9}\omega_1\omega_2}}{\frac{1}{3}\omega_1}, 1, 1 \right\}.$$

The solution to equation (A.2) is

$$\vec{P} = \sum_i c_i \hat{\varepsilon}_i \exp(-\lambda_i t),$$

where c_i is the coefficient that depends on the initial conditions and $\hat{\varepsilon}_i$ is the normalized eigenvector.

Assuming that after the radiofrequency pulse we have saturated the nuclear polarization only at site $\nu = 1$, while that at sites 2 and 3 remains unchanged, the initial conditions are

$$P^1(t=0) = 0, \qquad P^2(t=0) = P_0^2, \qquad P^3(t=0) = P_0^3. \tag{A.3}$$

Therefore the time evolution of nuclear polarization at site $\nu = 1$ is

$$P^1(t) - P_0^1 = -\frac{P_0^1}{2}(B_2\,\mathrm{e}^{-\lambda_2 t} + B_3\,\mathrm{e}^{-\lambda_3 t}), \tag{A.4}$$

where

$$B_{2,3} = 1 \pm (1 - \tfrac{7}{6}\mathrm{e}^{\alpha}((1 - \tfrac{7}{6}\mathrm{e}^{\alpha})^2 + \tfrac{2}{9}\mathrm{e}^{\alpha})^{-1/2} \tag{A.5}$$

with $\alpha = \Delta/RT$.

In figure A.1 the behaviour of B_i and λ_i $(i = 2, 3)$ as a function of α are shown. For $\alpha > 1$ the coefficient B_2 decreases exponentially, while the value of B_3 remains approximately constant with α. It is clear from figure A.1 that for $\Delta > RT$ the relaxation of the nuclear polarization can be described with a single exponential decay curve with a relaxation time $T_1^{-1} = \lambda_3 = \frac{40}{21}\omega_1$. According to this analysis, the parameter E_a, obtained by fitting the experimental data to equation (2), corresponds to the potential barrier of the lowest energy minimum.

References

[1] Crowe R W and Smith C P 1950 *J. Am. Chem. Soc.* **72** 1098

[2] Kushner L M, Crowe R W and Smith C P 1950 *J. Am. Chem. Soc.* **72** 1091

[3] Thorbjönsrud J, Ellestad O H, Klæboe P, Torgrimsen T and Christensen D H 1973 *J. Mol. Struct.* **17** 5

[4] Gustavsen J E, Klæboe P and Stölevik R 1978 *J. Mol. Struct.* **50** 285

[5] Farup P E and Stølevik R 1974 *Acta Chem. Scand.* A **28** 871
[6] Zuriaga M J, Monti G A and Martín C A 1991 *J. Phys.: Condens. Matter* **3** 2287
[7] Bishui B M 1953 *Indian J. Phys.* **27** 90
[8] Chihara H and Nakamura N 1981 *Advances in Nuclear Quadrupole Resonance* vol 4 (London: Heyden)
[9] Das T P and Hahn E L 1958 *Nuclear Quadrupole Resonance SpectroscopySolid State Physics* Suppl 1 (New York: Academic)
[10] Cohen M H and Reif F 1957 *Solid State Physics* vol 5 (New York: Academic) p 321
[11] Stoneham A M 1969 *Rev. Mod. Phys.* **41** 82
[12] Blinc R 1981 *Phys. Rep.* **79** 331
[13] Meriles C A, Perez S C, Wolfenson A E and Brunetti A H 1999 *J. Chem. Phys.* **110** 7392
[14] Bussandri A P, Zuriaga M J and Martin C A 1998 *J. Phys. Chem. Solids* **59** 201
[15] Hahn E L 1950 *Phys. Rev.* **80** 580
[16] Bussandri A P and Zuriaga M J 1998 *J. Magn. Reson.* **131** 224
[17] Martín C A 1982 *Proc. 7th Int. Conf. on Thermal Analysis* vol 1 (New York: Wiley) p 205
[18] Pope M I and Judd M D 1980 *Differential Thermal Analysis* (London: Heyden) p 49
[19] Adam G and Gibbs J H 1965 *J. Chem. Phys.* **43** 139
[20] Burger A and Ramberger R 1979 *Mikrochim. Acta* **2** 259
[21] Pies W and Weiss A 1981 *Z. Phys. Chem. Neue Folge* **127** 147
[22] Ostwald W 1897 *Z. Physik. Chem.* **22** 289
[23] Kushida T, Benedek G B and Bloembergen N 1956 *Phys. Rev.* **104** 1364
[24] Brown R J C 1960 *J. Chem. Phys.* **32** 116
[25] Bellows J C and Prasat P 1977 *J. Chem. Phys.* **66** 625
[26] Bellows J C and Prasat P 1978 *Chem. Phys. Lett.* **54** 439
[27] Caldarone B, Taiti C, Bini R and Schettino V 1995 *J. Chem. Phys.* **102** 6653
[28] Alexander S and Tzalmona A 1965 *Phys. Rev.* A **138** 845
[29] Ainbinder M E, Kjuntsel I A, Mokeeva V A, Osipenko A N, Soifer G B and Shaposnikov I G 1980 *J. Mol. Struct.* **58** 349
[30] Kiichi T, Nakamura N and Chihara H 1972 *J. Magn. Reson.* **6** 516